Electronic Supplementary Material (ESI) for Nanoscale.

Supporting Information:

Van der Waals Integration of Mixed-dimensional CeO_2@Bi Heterojunction for Plasma Enhanced High-performance Self-Powered Photodetector

Xinlin Liu[a], Cailing Liu[a], Yushuang Fu[a], Yiguo Xu[b*], Karim Khan[c], Ayesha Khan Tareen[c], and Ye Zhang[a*]

a. School of Chemistry and Chemical Engineering, University of South China, Hengyang 421001, China

E-mail: yezhang@usc.edu.cn

b. Academy for Advanced Interdisciplinary Studies, Southern University of Science and Technology, Shenzhen 518055, China

c. School of Mechanical Engineering, Dongguan University of Technology, Dongguan 523808, China

E-mail: yiguo.xu@outlook.com

Experimental Section
Material

Cerium nitrate hexahydrate ($Ce(NO_3)_3·6H_2O$, 99.99%) was provided by Adamas-beta. Bismuth nitrate pentahydrate ($Bi(NO_3)_3·5H_2O$, 99.99%), sodium hydroxide(NaOH, AR, 96%), poly(vinylidene fluoride) (PVDF, Mw ≈ 400,000 g mol^{-1}), ethylene glycol (EG, AR, 98%), dimethylformamide (DMF, AR, 99.5%) were provided by Shanghai Macklin Biochemical Co., Ltd. All chemical reagents are used without further purification.

Synthesis of Ceria nanorods (CeO_2 NRs)

The CeO_2 NRs were prepared according to the previously reported hydrothermal method.[1,2] Typically, 3.2 g NaOH was first dissolved in 13.3 mL DIW to form solution A, and 0.28 g $Ce(NO_3)_3·6H_2O$ was dissolved in 1.7 mL to form solution B. Then A and B were mixed and the mixture was stirred at room temperature for 30 min. After stirring, the mixed solution was transferred to a 25 mL Teflon reactor and placed in an electric oven at 100 °C for reacting 24 h. After the reactor cooled down to room temperature, the supernatant was removed through a pipe carefully, and the precipitate was washed by centrifuging (8000 rpm for 5 min) with DIW and ethanol for several times. The finally product was dried under vacuum oven at 60 °C overnight.

References:

1. M. Lykaki, E. Pachatouridou, S. A. Carabineiro, E. Iliopoulou, C. Andriopoulou, N. Kallithrakas-Kontos, S. Boghosian and M. Konsolakis, *Appl. Catal. B: Environ.*, 2018, **230**, 18-28.
2. Z.-J. Gong, Y.-R. Li, H.-L. Wu, S. D. Lin and W.-Y. Yu, *Appl. Catal. B: Environ.*, 2020, **265**, 118524.

Synthesis of Ceria nanorods@ Bismuth Quantum Dot van der Waals heterostructures (CeO_2@Bi vdWHs)

CeO_2@Bi vdWHs were prepared via a hydrothermal method. In a typical procedure, 0.17 g CeO_2 NRs were dispersed in 20 mL EG to form solution A. 0.49 g $Bi(NO_3)_3·5H_2O$ was dispersed in 30 mL EG to form solution B. Then A and B were mixed and the mixture was stirred for 30 min at room temperature to obtain a homogeneous solution. The mixture was transferred into a 100 mL Teflon reactor and placed in an electric oven at 180 °C for reacting 4 h. After the reactor cooled to room temperature, the supernatant was removed through a pipe carefully, and the

precipitate was washed with DIW and ethanol for several times through centrifuging (8000 rpm for 5 min). The final product was dried under vacuum oven at 60 °C overnight.

Preparation of CeO_2@Bi-based PDs

Herein, ITO glass was used as the substrate. At first, ITO glass was carefully cleaned with DIW, ethanol and acetone for each 10 min, respectively. Then the ITO glass was dried with nitrogen. 50 mg PVDF was dispersed in 100 mL of NMP and stirred for 24 h to obtain a homogeneous mixture. 3 mg CeO_2@Bi was dispersed in 1 mL PVDF/DMF solution, which was dropped onto the ITO substrate and kept in vacuum oven at 60 °C for 12 h to form CeO_2@Bi-based PDs.

Characterization

The morphologies of CeO_2 and CeO_2@Bi were studied by TEM (JEOL JEM F200). The UV-Vis absorption spectra were performed by a UV-2100 UV-Vis spectrophotometer (Shimadzu Scientific Instruments). The structures of CeO_2 and CeO_2@Bi were examined by the XRD spectrometer (scan rate of 6.25 min^{-1}), Raman spectroscopy (HORIBA Lab RAM HR800, 532 nm) and X-ray photoelectron spectroscopy (Thermo Scientific ESCALAB 250Xi).

Measurement of CeO_2@Bi vdWHs Photoresponse

The photoresponse of CeO_2@Bi-based PDs was studied through a PEC-type photodetection system. The CeO_2@Bi coated ITO glass, Pt wire, and Ag/AgCl were used as the working electrode, counter electrode, and reference electrode, respectively. KOH, KCl, and HCl with different concentrations were adopted as the electrolytes. The devices were irradiated by different wavelengths (350, 365, 400, 450, 500, 550, 600, and 650 nm), and the different power densities were classified as level I, II, III and IV (see **Table S1**). As a comparison, CeO_2 NRs and Bi QDs-based PDs were also studied as references. The LSV was carried out ranging from 0 to 1.0 V with the scan rate of 0.01 V s^{-1}. Amperometric current-time (I-t) measurements were performed under different bias potentials (0-0.6 V) with an interval of 0.02 s. The EIS spectra were performed ranging from 1 to 10^5 Hz with an amplitude of 0.005

V.

Computational methods

DFT calculations were performed with the Vienna ab initio simulation package (VASP) code.[1,2] The projector augmented wave (PAW) potential was used to describe electron–core interactions. The exchange-correlation energies were treated using the PBE functional of the generalized gradient approximation (GGA).[3] To avoid the self-interaction error caused by DFT that leads to over-delocalized electrons, DFT+U approach with U=5 for f states of Ce atoms was employed.[4] The Grimme's D3 method was chosen to describe vdW forces between CeO_2(111) and Bi layers.[5] The thickness of the vacuum layer was larger than 15 Å along z direction to prevent mirror interactions between adjacent supercells. The plane wave basis sets with cutoff energy of 520 eV was used for all calculations. The energy convergence criterion was set to be 10^{-6} eV, and the force on each atom was converged to smaller than 0.01 eV/Å during structure relaxation. The Brillouin zone of Bi, CeO_2(111) and CeO_2@Bi were sampled with 13×13×1, 13×13×1 and 7×7×1 Γ-centered k-mesh, respectively.

References:

1. G. Kresse and J. Furthmüller, *Phys. Rev. B*, 1996, **54**, 11169.
2. G. Kresse and J. Hafner, *Phys. Rev. B*, 1993, **47**, 558.
3. P. E. Blöchl, *Phys. Rev. B*, 1994, **50**, 17953.
4. S. L. Dudarev, G. A. Botton, S. Y. Savrasov, C. Humphreys and A. P. Sutton, *Phys. Rev. B*, 1998, **57**, 1505.
5. S. Grimme, J. Antony, S. Ehrlich and H. Krieg, *J. Chem. Phys.*, 2010, **132**, 154104.

Table S1. The applied P_λ of incident light with various wavelengths.

P_λ (mW cm^{-2})	I	II	III	IV
Simulated Light	134.3	410.0	679.0	832.0
350 nm	11.2	35.7	60.1	73.7
365 nm	0.9	4.8	8.4	10.3
380 nm	16.3	52.4	87.3	107.1
450 nm	15.5	52.0	87.3	107.2
500 nm	16.6	53.4	90.1	111.0
550 nm	15.6	50.7	85.9	105.3

600 nm	16.4	52.7	90.0	110.6
650 nm	13.4	43.7	73.0	90.1

The wavelengths of 365-650 nm are obtained from PLS-FX300HU light source with various optical filters.

Table S2. The typical values of P_{ph} and R_{ph} for pristine CeO_2, Bi, and CeO_2@ Bi-based PDs under the same experimental conditions at level III.

Materials	Electrolyte	Bias Potential (V)	Photocurrent ($\mu A\ cm^{-2}$)	Responsivity ($\mu A\ W^{-1}$)
CeO_2 NRs	1.0 M KOH	0.6	0.63	0.93
Bi QDs	1.0 M KOH	0.6	0.77	1.14
CeO_2@Bi	1.0 M KOH	0.6	39.64	58.38

Table S3. The comparison of CeO_2@Bi with other reported materials-based PEC-type photodetectors.

Materials	**Experimental conditions**	**Photocurrent ($\mu A\ cm^{-2}$)**	**Responsivity ($\mu A\ W^{-1}$)**	**t_{res}/t_{rec} (s)**	**Ref**
CeO_2@Bi	1.0 M KOH, 0.6 V	39.64	938.89	0.02/0.02	This work
Bi QDs	1.0 M KOH, 0.6 V	1.02	294.9	0.2/0.2	[1]
β-PbO QDs	0.01 M KOH, 0.4 V	7.27	4280	0.09-0.27/0.13-0.39	[2]
Te@Bi	0.5 M KOH, 0.6 V	16.87	142.97	0.09/0.09	[3]
Bi_2O_2S NSs	1.0 M KOH, 0.6 V	61.2	13×10^3	0.01/0.045	[4]
B NSs	0.3 M KOH, 0.6 V	0.62	91.7	0.1/0.2	[5]
InSe	0.3 M KOH, 0 V	42.55	10.14×10^3	0.002/0.037	[6]
AlGaN:Ru	0.01 M H_2SO_4, 0 V	55	48.8×10^3	0.083/0.019	[7]
BP NSs	0.1 M KOH, 0.6 V	0.642	5.4	0.5/1.1	[8]
Bi_2S_3 NSs	0.1 M KOH, 0.6 V	42	210	0.1/0.1	[9]
InSe	0.2 M KOH, 1.0 V	0.3255	4.9	5	[10]
PbO NSs	0.1 M KOH, 0.4 V	29.55	1273.11	0.1/0.1	[11]
Te NSs	0.1 M KOH, 0.6 V	0.136	13.4	0.0545/0.0702	[12]
β-Ga_2O_3 NRAs	0.5 M Na_2SO_4, 0 V	14.82	3810	0.076/0.056	[13]
Se NFs	0.1 M KOH, 0.6 V	1.28	10.45	-	[14]
GeSe NSs	0.5 M KOH, 0.6 V	7.1	2304	0.2/0.3	[15]
PbS NPLs	0.1 M KOH, 0.4 V	12.89	10970	0.16/-	[16]

Graphdiyne	0.1 M KOH, 0.6 V	5.98	50.67	-	[17]
PbSe	0.1 M KOH, 0.4 V	11.88	12370	0.12/0.13	[18]

References:

1. C. Xing, W. Huang, Z. Xie, J. Zhao, D. Ma, T. Fan, W. Liang, Y. Ge, B. Dong, J. Li and H. Zhang, *ACS Photonics*, 2017, **5**, 621-629.
2. W. Huang, X. Jiang, Y. Wang, F. Zhang, Y. Ge, Y. Zhang, L. Wu, D. Ma, Z. Li, R. Wang, Z. N. Huang, X. Dai, Y. Xiang, J. Li and H. Zhang, *Nanoscale*, 2018, **10**, 20540-20547.
3. Y. Zhang, F. Zhang, L. Wu, Y. Zhang, W. Huang, Y. Tang, L. Hu, P. Huang, X. Zhang and H. Zhang, *Small*, 2019, **15**, e1903233.
4. X. Yang, L. Qu, F. Gao, Y. Hu, H. Yu, Y. Wang, M. Cui, Y. Zhang, Z. Fu, Y. Huang, W. Feng, B. Li and P. Hu, *ACS Appl. Mater. Interfaces*, 2022, **14**, 7175-7183.
5. D. Ma, R. Wang, J. Zhao, Q. Chen, L. Wu, D. Li, L. Su, X. Jiang, Z. Luo, Y. Ge, J. Li, Y. Zhang and H. Zhang, *Nanoscale*, 2020, **12**, 5313-5323.
6. X. Yang, X. Liu, L. Qu, F. Gao, Y. Xu, M. Cui, H. Yu, Y. Wang, P. Hu and W. Feng, *ACS Nano*, 2022, **16**, 8840-8848.
7. D. Wang, C. Huang, X. Liu, H. Zhang, H. Yu, S. Fang, B. S. Ooi, Z. Mi, J. H. He and H. Sun, *Adv. Opt. Mater.*, 2021, **9**, e2000893.
8. X. Ren, Z. Li, Z. Huang, D. Sang, H. Qiao, X. Qi, J. Li, J. Zhong and H. Zhang, *Adv. Funct. Mater.*, 2017, **27**, e1606834.
9. W. Huang, C. Xing, Y. Wang, Z. Li, L. Wu, D. Ma, X. Dai, Y. Xiang, J. Li, D. Fan and H. Zhang, *Nanoscale*, 2018, **10**, 2404-2412.
10. Z. Li, H. Qiao, Z. Guo, X. Ren, Z. Huang, X. Qi, S. C. Dhanabalan, J. S. Ponraj, D. Zhang, J. Li, J. Zhao, J. Zhong and H. Zhang, *Adv. Funct. Mater.*, 2018, **28**, e1705237.
11. C. Xing, X. Chen, W. Huang, Y. Song, J. Li, S. Chen, Y. Zhou, B. Dong, D. Fan, X. Zhu and H. Zhang, *ACS Photonics*, 2018, **5**, 5055-5067.
12. Z. Xie, C. Xing, W. Huang, T. Fan, Z. Li, J. Zhao, Y. Xiang, Z. Guo, J. Li, Z. Yang, B. Dong, J. Qu, D. Fan and H. Zhang, *Adv. Funct. Mater.*, 2018, **28**, e1705833.
13. K. Chen, S. Wang, C. He, H. Zhu, H. Zhao, D. Guo, Z. Chen, J. Shen, P. Li, A. Liu, C. Li, F. Wu and W. Tang, *ACS Appl. Nano Mater.*, 2019, **2**, 6169-6177.
14. T. Fan, Z. Xie, W. Huang, Z. Li and H. Zhang, *Nanotechnology*, 2019, **30**, 114002.
15. D. Ma, J. Zhao, R. Wang, C. Xing, Z. Li, W. Huang, X. Jiang, Z. Guo, Z. Luo, Y. Li, J. Li, S. Luo, Y. Zhang and H. Zhang, *ACS Appl. Mater. Inter.*, 2019, **11**, 4278-4287.
16. L. Gao, H. Chen, R. Wang, S. Wei, A. V. Kuklin, S. Mei, F. Zhang, Y. Zhang, X. Jiang, Z. Luo, S. Xu, H. Zhang and H. Agren, *Small*, 2021, **17**, e2005913.
17. Y. Zhang, P. Huang, J. Guo, R. Shi, W. Huang, Z. Shi, L. Wu, F. Zhang, L. Gao, C. Li, X. Zhang, J. Xu and H. Zhang, *Adv. Mater.*, 2020, **32**, e2001082.
18. L. Gao, R. Wang, A. V. Kuklin, H. Zhang and H. Ågren, *Adv. Funct. Mater.*, 2021, **31**, e2010401.

Table S4. The details of P_{ph} and R_{ph} of PD under different wavelength at 0.6 V in 1.0 M KOH solution.

Materials	Bias potential (V)	Electrolyte	Wavelength (nm)	Photocurrent (μA cm^{-2})				Responsivity (μA W^{-1})			
				I	II	III	IV	I	II	III	IV
CeO_2@ Bi	0.6 V	1.0 M KOH	350 nm	1.15	2.98	4.91	6.18	103.12	83.33	81.70	83.85
			365 nm	0.84	2.54	4.69	6.32	938.89	529.17	558.93	614.08
			380 nm	0.78	2.48	4.93	6.44	47.55	47.42	56.47	60.13
			450 nm	0.23	0.76	1.37	1.84	14.84	14.52	15.75	15.27

Table S5. The details of P_{ph} and R_{ph} of PD under different wavelength at 0.6 V in 0.1 M KOH solution.

Materials	Bias potential (V)	Electrolyte	Wavelength (nm)	Photocurrent (μA cm^{-2})				Responsivity (μA W^{-1})			
				I	II	III	IV	I	II	III	IV
CeO_2@ Bi	0.6 V	0.1 M KOH	350 nm	0.48	1.22	1.76	1.91	42.86	34.31	29.37	25.92
			365 nm	0.46	1.13	1.55	1.61	505.56	236.46	185.12	155.83
			380 nm	0.30	0.88	1.41	1.65	18.40	16.89	16.09	15.41
			450 nm	0.17	0.63	1.00	1.13	8.04	13.27	11.45	10.54

Table S6. The details of P_{ph} and R_{ph} of PD under different wavelength at 0.6 V in 0.5 M KOH solution.

Materials	Bias potential (V)	Electrolyte	Wavelength (nm)	Photocurrent (μA cm^{-2})				Responsivity (μA W^{-1})			
				I	II	III	IV	I	II	III	IV
CeO_2@ Bi	0.6 V	0.5 M KOH	350 nm	0.55	1.39	2.11	2.35	49.11	38.94	35.11	31.89
			365 nm	0.60	1.44	2.08	2.32	666.67	300.00	247.62	225.73
			380 nm	0.50	1.22	1.95	2.15	30.80	23.30	22.39	20.08

	450 nm	0.21	0.66	1.01	1.14	8.43	12.70	11.56	10.68

Table S7. The values of P_{ph} and R_{ph} of CeO_2@Bi-based self-powered PD with different wavelengths in 0.1 M KOH electrolyte.

Materials	Electrolyte	Wavelength (nm)	Photocurrent (μA cm^{-2})				Responsivity (μA W^{-1})			
			I	II	III	IV	I	II	III	IV
CeO_2@Bi	1.0 M KOH	350 nm	0.[illegible]	0.[illegible]	0.56	0.37	50.00	20.24	9.27	4.96
		365 nm	0.[illegible]	0.[illegible]	0.59	0.34	643.61	160.47	69.94	32.38
		380 nm	0.[illegible]	0.[illegible]	0.21	0.15	7.72	4.18	2.33	1.34
		450 nm	0.[illegible]	0.[illegible]	0.27	0.22	8.23	4.94	3.05	2.07

Table S8. The values of P_{ph} and R_{ph} of CeO_2@Bi-based self-powered PD with different wavelengths in 0.5 M KOH electrolyte.

Materials	Electrolyte	Wavelength (nm)	Photocurrent (μA cm^{-2})				Responsivity (μA W^{-1})			
			I	II	III	IV	I	II	III	IV
CeO_2@Bi	1.0 M KOH	350 nm	0.[illegible]	1.[illegible]	0.62	0.51	67.86	32.57	20.55	13.77
		365 nm	0.[illegible]	1.[illegible]	0.77	0.15	766.11	219.69	91.64	14.76
		380 nm	0.[illegible]	0.[illegible]	0.34	0.24	21.41	7.64	3.83	2.25
		450 nm	0.[illegible]	0.[illegible]	0.10	0.10	3.67	2.05	1.16	0.96

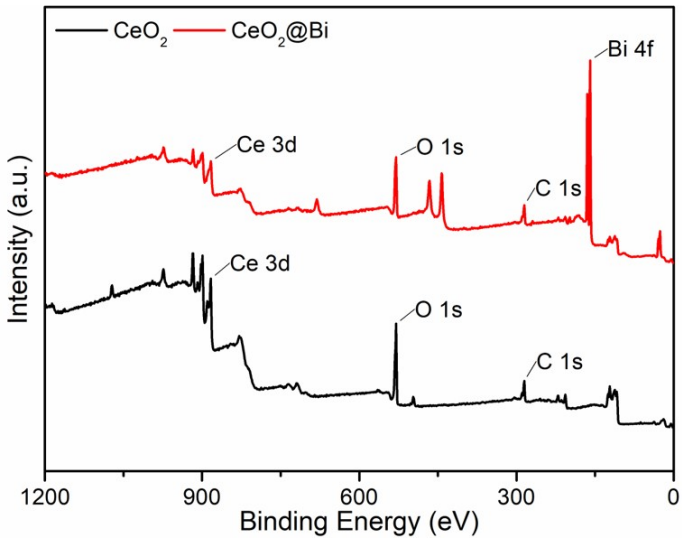

Figure S1. The survey spectrum of CeO_2 and CeO_2@Bi heterojunctions.

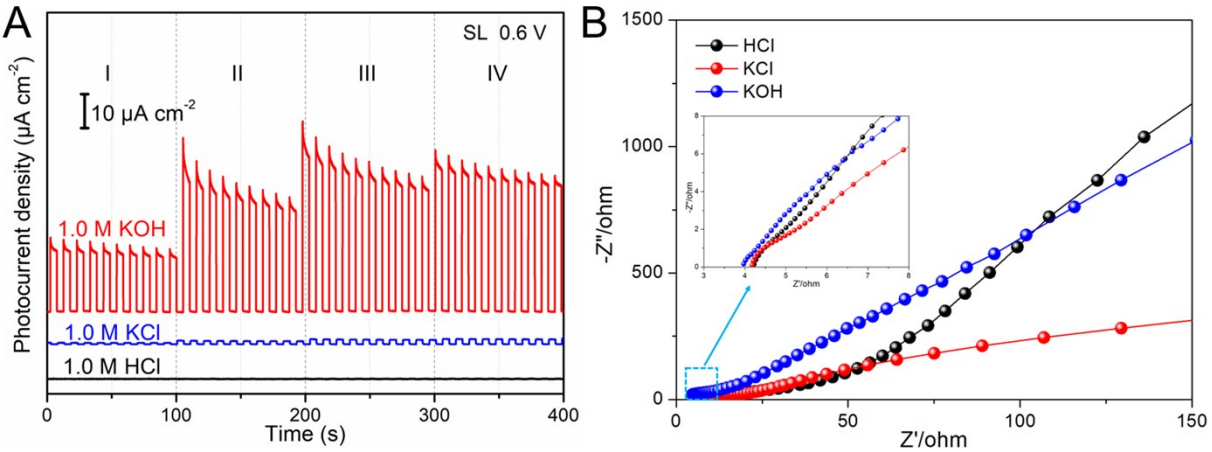

Figure S2. The photodetection behaviors and the EIS spectra of CeO_2@Bi-based photodetetor in different electrolytes.

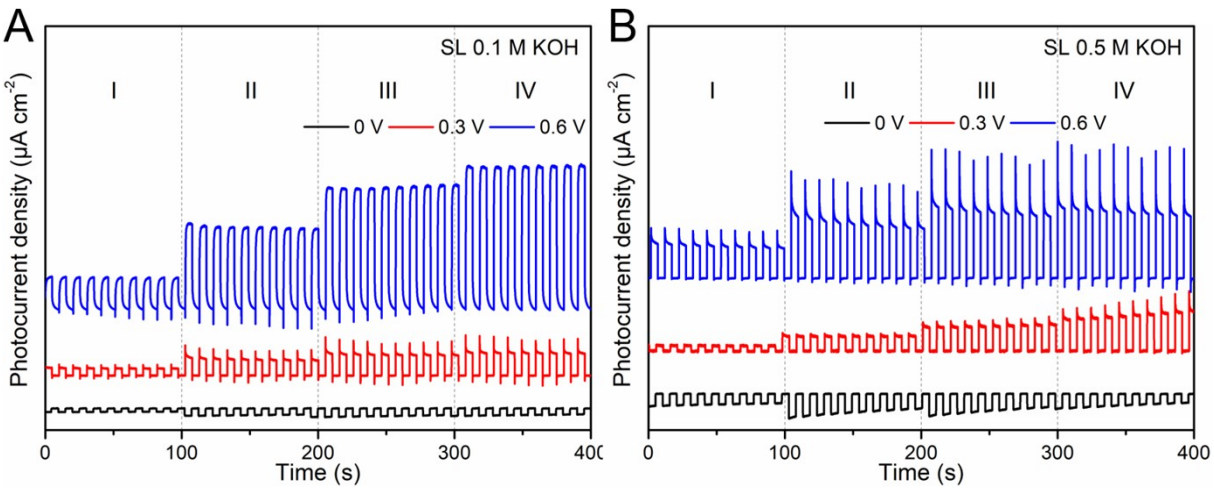

Figure S3. The photodetection behaviors at 0.1 and 0.5 M KOH electrolytes with different bias potentials.

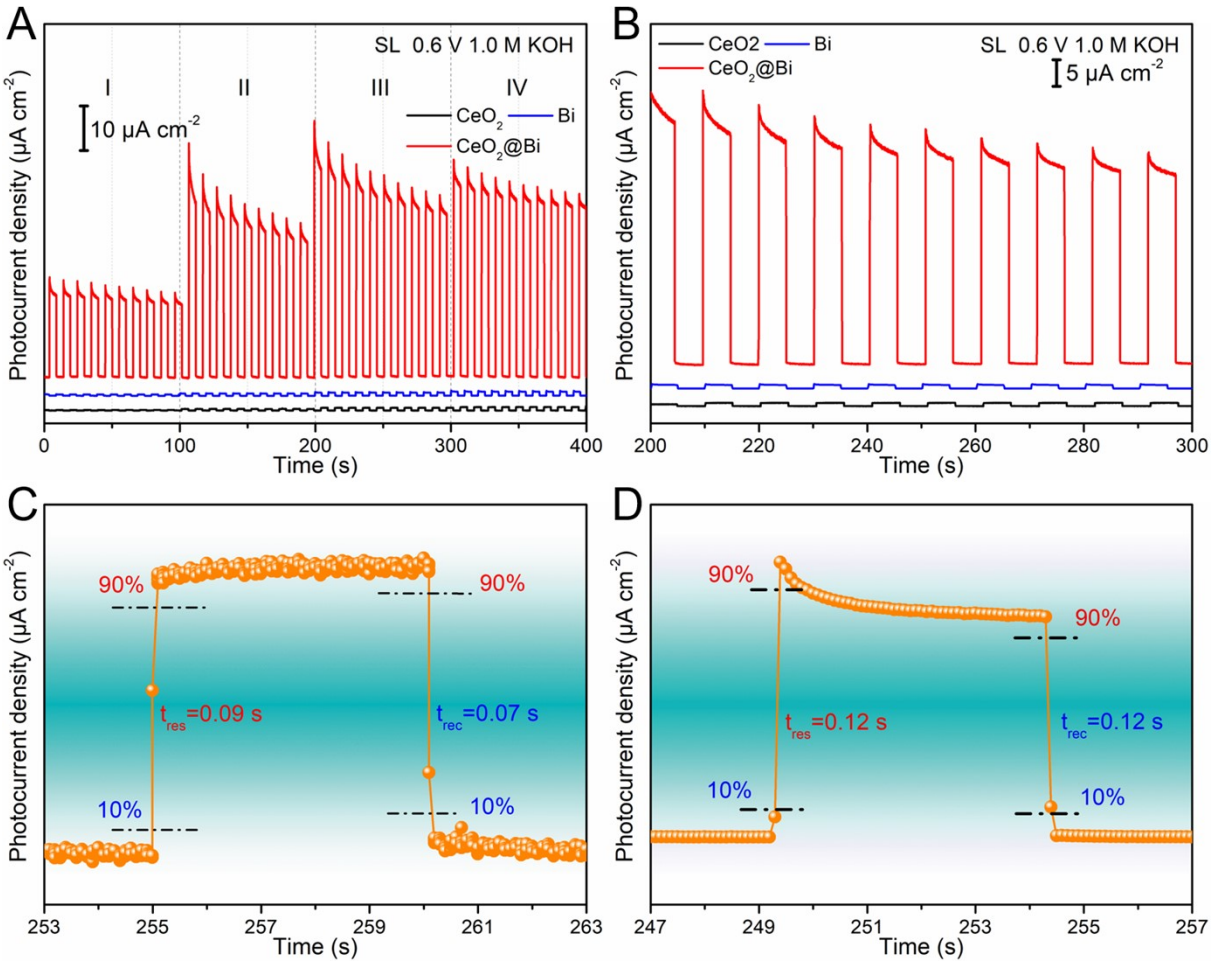

Figure S4. (**A**) The photodetection behaviors of pristine CeO_2 NRs, Bi QDs and CeO_2@Bi-based PDs in 0.5 M KOH electrolyte at 0.6 V. (**B**) The details ON/OFF switching signals acquired level III from A. (**C-D**) The t_{res}/t_{rec} of pristine CeO_2 NRs and Bi QDs-based PD.

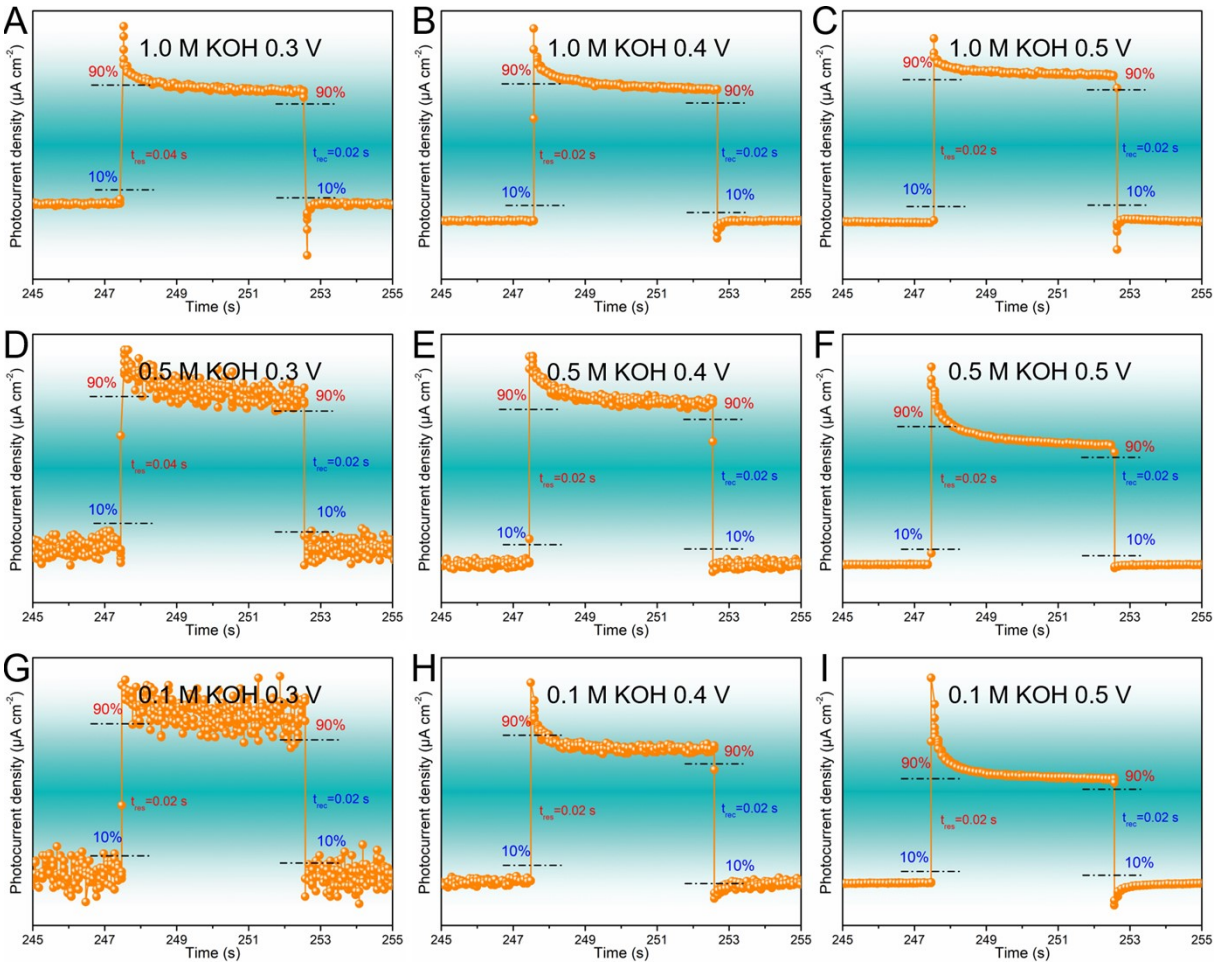

Figure S5. The t_{res}/t_{rec} of CeO_2@Bi-based PDs in (**A-C**) 1.0 M KOH electrolyte with different bias potentials, (**D-F**) 0.5 M KOH electrolyte with different bias potentials, and (**G-I**) 0.1 M KOH electrolyte with different bias potentials.

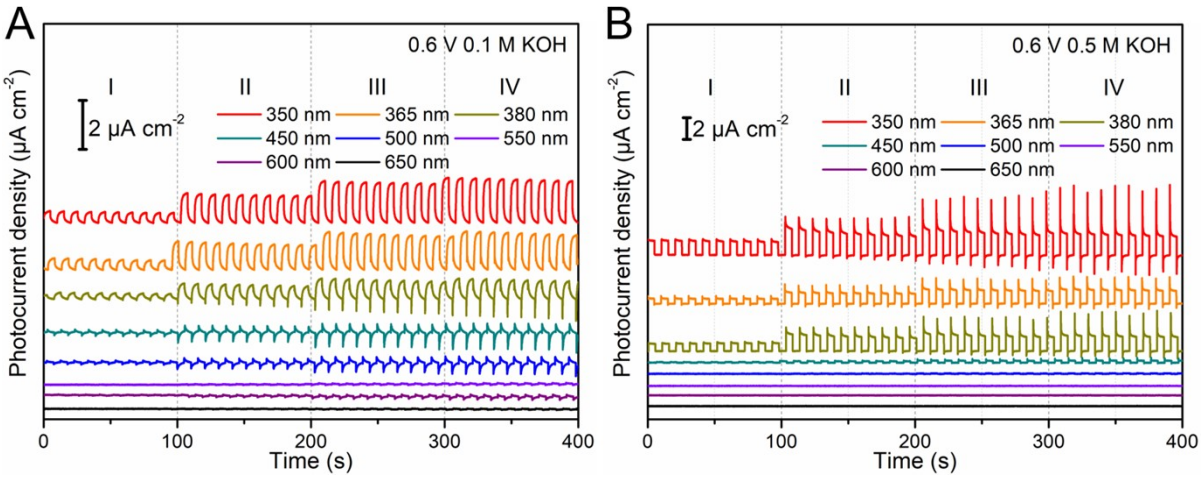

Figure S6. The photodetection behaviors at 0.1 and 0.5 M KOH electrolytes and 0.6 V with different wavelengths illumination.

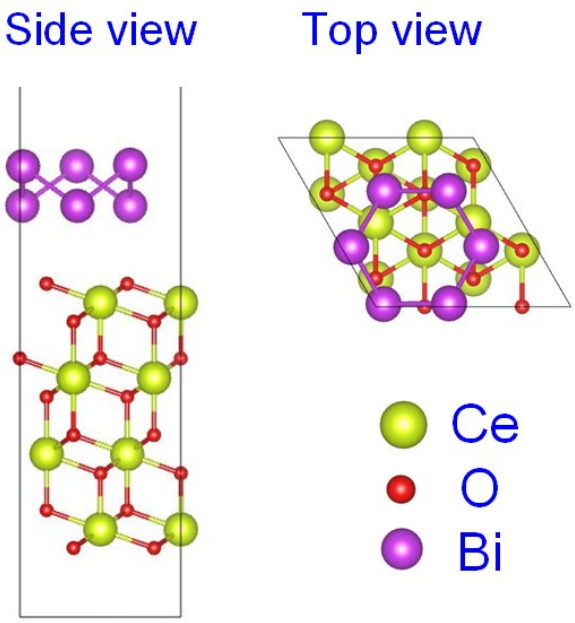

Figure S7. Side and top views of the optimized structures of CeO_2@Bi vdWH.

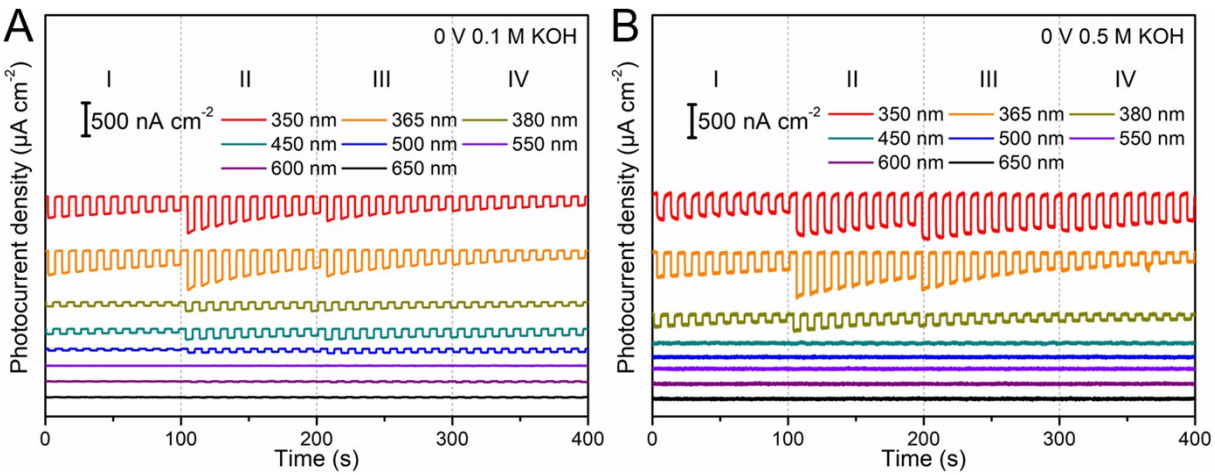

Figure S8. The self-powered photodetection behaviors of CeO_2@Bi-based PD in 0.1 and 0.5 M KOH electrolytes under different wavelength illumination.